Applied Thermal Engineering 228 (2023) 120436

Contents lists available at ScienceDirect

Applied Thermal Engineering

journal homepage: www.elsevier.com/locate/apthermeng

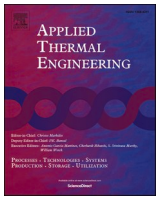

Research Paper

Modeling and parametric optimization of a liquid piston compressor with inner cooling tubes

N. Cerkovnik [a], V.A.F. Costa [b], A.M.G. Lopes [c,*]

[a] University of Ljubljana, Faculty of Mechanical Engineering, Ljubljana, Slovenia
[b] Centro de Tecnologia Mecânica e Automação e Departamento de Engenharia Mecânica da Universidade de Aveiro, Campus Universitário de Santiago, 3810-193 Aveiro, Portugal
[c] Univ Coimbra, ADAI, Departamento de Engenharia Mecânica, Rua Luís Reis Santos, Pólo II, 3030-788 Coimbra, Portugal

ARTICLE INFO

Keywords:
Liquid piston (LP)
Compressed air energy storage (CAES)
Near-isothermal compression
Inserted cooling tubes
Heat transfer
Computational fluid dynamics (CFD)

ABSTRACT

This work proposes a new configuration of liquid piston compressors and a methodology for their optimization, with special attention to heat removal from the compressing gas, in order to minimize the mechanical work required for the compression process. The adopted approach starts with the solution of the governing equations through a 0D model (lumped approach). A new correlation for the heat transfer coefficient is presented to calculate the sensible heat transfer from the compressing gas to the cooling liquid. The results of the 0D model are validated by comparison with experimental and numerical data from the literature and with performed CFD calculations. In the proposed geometric configuration, heat is removed from the compressing gas through a tubes bundle inserted in the compression chamber, the liquid cooling medium flowing inside the tubes. This geometric configuration was chosen because it is simple to design and common materials and manufacturing processes can be used for its manufacturing. In addition, no regeneration of the inserts is required from cycle to cycle, making that configuration ideal for cyclic operation. The parametric study performed focuses on the dependence of the overall efficiency on the number and diameter of the cooling tubes and the speed of the liquid piston. It is found that the overall efficiency is highest for a given number of tubes with at a specific diameter, and that the combination of a few cooling tubes with a larger diameter and a higher piston speed gives the best overall efficiency.

1. Introduction

To avoid the threat of climate change posed by increasing greenhouse gases emissions due to rising energy consumption, priority must be given to the development of new low or zero-carbon energy technologies [1]. It is important to develop not only technologies to produce cleaner energy, but also technologies to store, process, and distribute it. Energy demand is higher than ever and will continue increasing as development continues. Many countries around the world are trying to make the transition to a greener and less polluting future. To this end, conventional energy sources are being replaced with renewable energy. The main problem with this is that their availability does not match energy demand or use, so requiring energy storage.

Although compressed air is a promising option for storing energy from renewable sources, more efficient methods of compressing air are needed. Mechanical gas compressors are the most common solution today. Although they are still being extensively researched, they are not as efficient as desired. Their main problems are energy losses due to the friction of metal and rubber parts, internal leakage through the sealing elements, and the compression induced air temperature increase. The result of compression is therefore hot compressed gas, whose thermal energy is usually lost when it is cooled during storage before use, thus reducing the overall efficiency of compressed air energy storage systems (CAES). Additionally, as hydrogen becomes more widely used as an energy carrier its low density requires high storage pressures, research into more efficient compressors will become even more challenging. The energy required to compress a gas can be reduced if the gas is cooled during compression. The so-called liquid piston compressors (LPCs) are therefore an advantageous alternative to the usual mechanical (solid piston) compressors. The absence of moving parts, null internal leakage, and the ability to provide adequate geometry for gas compression and improved heat release from the gas during compression are key advantages of LPCs.

* Corresponding author.
E-mail addresses: nejc.cerkovnik@fs.uni-lj.si (N. Cerkovnik), v.costa@ua.pt (V.A.F. Costa), antonio.gameiro@dem.uc.pt (A.M.G. Lopes).

https://doi.org/10.1016/j.applthermaleng.2023.120436
Received 2 September 2022; Received in revised form 8 March 2023; Accepted 17 March 2023
Available online 23 March 2023

Nomenclature:

Abbreviations:

0D	Zero dimensions
CAES	Compressed air energy storage
CFD	Computational Fluid Dynamics
CR	Compression Ratio
LES	Large Eddy Simulation
LPC	Liquid Piston Compressor
PISO	Pressure Implicit with Splitting Operators
WALE	Wall Adapting Local Eddy-viscosity
VOF	Volume of Fluid

Greek symbols:

η	efficiency (-)
μ	dynamic viscosity (kg m^{-1} s^{-1})
ρ	density (kg m^{-3})

Non dimensional numbers:

Co	Courant number (-)
Nu	Nusselt number (-)
Pr	Prandtl number (-)
Re	Reynolds number (-)

Latin symbols:

A	surface (m^2)
c	heat capacity (J kg^{-1} K^{-1})
D	diameter (m)
d	tubes/pipes diameter (m)
f	friction factor (-)
h	heat transfer coefficient (W m^{-2} K^{-1}) / enthalpy (kJ kg^{-1})
h	specific enthalpy (kJ kg^{-1})
k	thermal conductivity (W m^{-1} K^{-1})
L	length (m)
m	mass (kg)
$\dot{m}$	mass flow rate (kg s^{-1})
N	number of cooling pipes / tubes (-)
$\dot{Q}$	Heat transfer rate (W)
P	perimeter (m)
p	pressure (Pa)
R	particular gas constant (J kg^{-1} K^{-1})
T	temperature (K)
t	time (s)
u	specific internal energy (J kg^{-1} K^{-1})
V	volume (m^3)
$\dot{V}$	volume flow rate (m^3 s^{-1})
v	velocity (m s^{-1})
W	mechanical work (J)
$\dot{W}$	work flow rate/power (W)
z	longitudinal position (m)

Subscripts:

0	initial
a	actual
atm	atmospheric
ch	cylinder head
cf	cooling fluid
cont	contact
cw	cylinder wall
f	friction
fin	final
g	gas
gl	gas–liquid
hyd	hydraulic
i	time instant
in	inlet
iso	isothermal
l	liquid
out	outlet
p	pipes/tubes, at constant pressure
pw	pipe/tube wall
v	at constant volume

The LPC, usually of cylindrical shape, is a simple device for compressing gases. A forced growing column of liquid pushes the gas upward in a closed chamber, increasing the gas pressure. The sealing of the gas is perfectly achieved by the liquid underneath. Since there are no other moving parts, sliding friction is absent even if viscous (liquid and gas) losses are increased. High compression ratios can be achieved and many gases can be compressed, making the LPC useful for hydrogen [2,3] and other specific industrial applications [4,5]. The efficiency of LPC is affected by the compression speed and compression ratio, decreasing at higher compression speeds and compression ratios [6,7]. The geometry of a cylinder, more specifically a high length to bore diameter (L/D) ratio, also increases the LPC efficiency. Another important advantage is that the liquid piston self-adapts to any compression chamber shape. Therefore, it is justified to build more efficient compression chamber shapes [8], moreover, inserts can be placed inside the compression chamber. As a result, the gas wall contact area to volume ratio can be greatly increased, with the corresponding benefits for the heat release (gas cooling) during compression, bringing the compression process closer to the ideal isothermal compression. Increasing the surface area to volume ratio was also the main goal of Van de Ven's research [9], in which it was shown that the use of liquid pistons can reduce energy consumption by 19% compared to solid (reciprocating) pistons. In that study, multiple small tubes were introduced into the cylindrical compression chamber to promote heat transfer from the compressing gas.

Some complex aspects of LPCs also need to be addressed here. Since the liquid and gas are in contact with each other under high pressure, there is a possibility of air entering the liquid, leading to additional losses and potential operation problems. It is important to create as well-defined separation between the liquid and gas as possible, to prevent liquid splashing by slow compression, or even using bladder to separate the two media. Several approaches to promote heat transfer besides [9] were investigated in the relevant literature, including the insertion of metal wires [10], porous media [11], thin metal plate structures [12], spray injection [8,13], aquatic foam [14], and the use of hollow spheres [15] in the compression chamber. All these approaches are promising to increase the efficiency of one compression cycle, but there is no information provided in these references on how to efficiently regenerate such inserts and quickly prepare the LPC for the next compression cycle. In addition, no optimization procedures were described for finding the optimal geometry and operating parameters.

The present work proposes the use of cooling tubes (in which flows the cooling medium) in the LPC compression chamber to extract heat from the gas during compression, thus keeping the outer walls of the tubes at a nearly constant low temperature. The cooling fluid is thermally regenerated by cooling it down in a heat exchanger. In addition, the arrangement of the tubes with their walls promotes heat transfer as in [9], resulting in a near isothermal gas compression. Such a LPC would be easy to construct, the inserted cooling tubes used do not need to be thermally regenerated from one compression cycle to the next, the obtained results indicating an increased compression performance. The disadvantages of the proposed and studied concept compared to other

listed solutions are: 1) the volume occupied by the cooling tubes, which reduces the usable/effective volume of the compression chamber, and 2) the mechanical energy required to circulate the cooling fluid (water). This leads to an optimization problem where main parameters are the number and diameter of the cooling tubes and the cooling liquid flow rate. The objective is to maximize the heat release from the compressing gas without greatly increasing the total mechanical work required for the compression process (gas compression + cooling fluid circulation). Parametric optimization process with 0D model is presented, that can be directly applied to LPC design and testing in industry and in energy storage solutions development and production.

2. Methods

2.1. Problem statement

A cylindrically shaped geometry is initially filled with gas at ambient temperature, as shown schematically in Fig. 1a. At the beginning of the compression cycle, liquid is pumped into the compression chamber and its column height increases, causing the gas pressure and temperature to rise. The cooling tubes inside the compression chamber (Fig. 1b) cool down the gas as it is being compressed, reducing the mechanical work required for the compression process. When the prescribed discharge pressure is reached, the valve at the top of the compression chamber opens and the gas is discharged under the displacement action of the liquid piston. After the gas is discharged, a suction process takes place. The suction process is not modelled in this work as it is assumed that gravity does all the suction work and no external work is required, which would result in lower compression efficiency.

2.2. Thermodynamic model

The compression and cooling processes are in a first approach modelled as a 0D problem compatible with the thermodynamic approach, which assumes uniform temperature and pressure in the gas and liquid domains. The gas compression and cooling are governed by the energy balance equation for a closed system,

$$\frac{dU_g}{dt} = \dot{W} + \dot{Q} \tag{1}$$

where U_g is the gas internal energy and $\dot{W}$ and $\dot{Q}$ are the work and the heat flow rates, respectively. The work flow rate (or mechanical power) can be expressed as:

$$\dot{W} = -p_g \frac{dV_g}{dt} \tag{2}$$

where p is the pressure and the subscript g designates the compressing gas. Characteristics of heat transfer inside compression chamber are quite complex. Three main heat transfer processes can be identified [16]: 1. Heat transfer from gas to liquid, which are in direct contact ($\dot{Q}_{gl}$), 2. Convection heat transfer from gas to cylinder walls ($\dot{Q}_{cw}$) and 3. Convection heat transfer from gas to the cooling pipes walls ($\dot{Q}_{pw}$). The total heat flow rate can be written as:

$$\dot{Q} = h_{g,gl} A_{\text{cont,gl}} \left(T_l - T_g\right) + h_{g,cw} A_{\text{cont,cw}} \left(T_{cw} - T_g\right) + h_{g,pw} A_{\text{cont,pw}} \left(T_{pw} - T_g\right) \tag{3}$$

where A_{cont} is the contact surface area between two instances on which heat transfer is active and h_g is the gas convection heat transfer coefficient. Both the contact surface area and the convection heat transfer coefficient evolve with time as liquid piston moves upwards and compresses the gas.

Considering the ideal gas behaviour, the time rate of change of the gas internal energy can be expressed as:

$$\frac{dU_g}{dt} = m_g c_v \frac{dT_g}{dt} \tag{4}$$

m_g and c_v being respectively the mass and the constant volume specific heat of the gas. Combining Eqs. (1) to (4) yields:

$$m_g c_v \frac{\mathrm{d}T_g}{\mathrm{d}t} = \dot{Q} - p_g \frac{dV_g}{dt} \tag{5}$$

For an ideal gas:

$$c_v = c_p - R \tag{6}$$

where R is the particular (specific) gas constant and c_p is the gas constant pressure specific heat. Eq. (5) can be rearranged to express the time derivative of the gas temperature

$$\frac{\mathrm{d}T_g}{\mathrm{d}t} = \left(\frac{1}{m_g \left(c_p - R\right)}\right)\left(\dot{Q} - p_g \frac{\mathrm{d}V_g}{\mathrm{d}t}\right) \tag{7}$$

As long as no too high pressure is reached, it can be related with temperature using the Ideal Gas Law.

$$p_g = \frac{m_g R T_g}{V_g} \tag{8}$$

Assuming that the walls of the cooling tubes are thin, or that the compressing gas and the cooling liquid are in direct contact, the gas temperature increase during compression results on heat transferred to the cooling and working liquids, and thermal energy is stored in the cylinder or tube walls. To model the temperature rise in the cooling media, we consider it as a separate region where the energy balance equation for an open system can be used. It should be noted that the available volume for air in the compression chamber is now reduced by

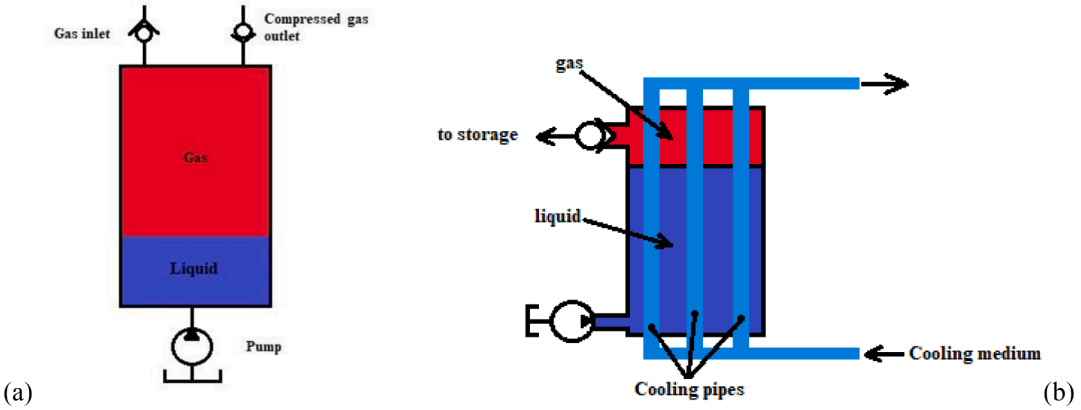

Fig.1. (a) Simple LPC, and (b) LPC with inner cooling tubes.

the cooling tubes. Again, pressure and temperature in cooling fluid domain is assumed to be uniform.

$$\frac{dU_{cf}}{dt} = \dot{W} + \dot{Q} + \dot{m}_{cf,in} h_{cf,in} - \dot{m}_{cf,out} h_{cf,out} \tag{9}$$

where $\dot{m}_{cf}$, h_{cf} are the cooling fluid mass flow rate and specific enthalpy, respectively. Subscripts *in* and *out* refer their values at the inlet and outlet of the cooling pipe. It is $\dot{W} = 0$ as the system does not produce or receive any mechanical work (incompressible cooling fluid), and mass balance equation for the cooling fluid gives:

$$\dot{m}_{cf,in} = \dot{m}_{cf,out} = \dot{m}_{cf} \tag{10}$$

Time derivative of cooling fluid temperature can be written as:

$$\frac{\mathrm{d}T_{cf}}{\mathrm{d}t} = \left(\frac{1}{m_{cf}\, c_{v,cf}}\right)\left(\dot{Q}_{pw} + \dot{m}_{cf}\left(h_{cf,in} - h_{cf,out}\right)\right) \tag{11}$$

$\dot{Q}_{pw}$ is the heat flow rate transferred from the compressing gas to the pipes walls under assumption of thin walls, which is thus equal to the heat transfer rate transferred directly to the cooling liquid, obtained from equation Eq. (3). Specific enthalpy of the cooling fluid is obtained at states:

$$h_{cf,in}\left(T_{cf,in}, p_{cf,in}\right) \tag{12}$$

$$h_{cf,out}\left(T_{cf,out}, p_{cf,out}\right) \tag{13}$$

The value of $T_{cf,in}$ is set as the boundary condition of unheated cooling water and $T_{cf,out}$ as:

$$T_{cf,out} = 2\,T_{cf} - T_{cf,in} \tag{14}$$

Assuming that the essentially uniform temperature of the cooling liquid in the studied domain is the average of its inlet and outlet temperatures (an assumption is further validated through CFD calculations in section 3.3).

For the numerical solution of temperature, Eqs. (7) and (11) are time-discretized and then solved with the forward Euler method (Eqs. (17) and (18)).

$$\left(\frac{\mathrm{d}T_g}{\mathrm{d}t}\right)_{i-1} = \left(\frac{1}{m_g\left(c_p - R\right)}\right)\left(\dot{Q}_{i-1} - p_{g,i-1}\frac{V_{g,i-2} - V_{g,i-1}}{\Delta \mathrm{t}}\right) \tag{15}$$

$$\left(\frac{\mathrm{d}T_{cf}}{\mathrm{d}t}\right)_{i-1} = \left(\frac{1}{m_{cf}\, c_{v,cf}}\right)\left(\dot{Q}_{i-1} + \dot{m}_{cf}\left(h_{cf,in} - h_{cf,out,i-1}\right)\right) \tag{16}$$

$$T_{g,\,i} = T_{g,\,i-1} + \Delta \mathrm{t}\left(\frac{\mathrm{d}T_g}{\mathrm{d}t}\right)_{i-1} \tag{17}$$

$$T_{cf,\,i} = T_{cf,\,i-1} + \Delta \mathrm{t}\left(\frac{\mathrm{d}T_{cf}}{\mathrm{d}t}\right)_{i-1} \tag{18}$$

The *new* pressure value is then calculated as:

$$p_{g,i} = \frac{m_g\, R\, T_{g,i}}{V_{g,\mathrm{i}}} \tag{19}$$

where Δt is the time step and i the time instant. For sufficiently small time step, the Euler method is a simple and stable way to study temperature and pressure time evolutions.

2.3. Compression chamber heat transfer

The evaluation of the convection heat transfer coefficient between the walls and the compressing air is a challenging problem. Due to the changing gas pressure and temperature, as well as the non-uniformities in the temperature and velocity field of the gas [17], the hydrodynamic instabilities and flow regimes [18], and the changing volume and surrounding wall contact area, there is no universal equation/correlation that can be used [19]. A simplifying assumption is to consider the situation under analysis as analogous to the fully developed flow in a pipe. Many of the available correlations have been developed for this situation and express the forced convection Nusselt number as a function of the Reynolds and Prandtl numbers:

$$Nu = A\, Re^{a}\, Pr^{b} \left(\frac{\mu}{\mu_0}\right)^{c} \tag{20}$$

where μ is the fluid dynamic viscosity. Constants A, a, b and c depend on the specific correlation and on the flow regime and type of inserts (constants for many models can be found in [18,19]). Once known the Nusselt number, the convection heat transfer coefficient is easily obtained as:

$$h = \frac{Nuk}{D} \tag{21}$$

where D is the characteristic dimension and k the gas thermal conductivity.

After an extensive study using correlations from [9,18-21], the Wochini [22] correlation for compression phase in internal combustion engines was chosen because it has the advantage that velocity, temperature, pressure, and bore diameter can be entered directly, eliminating the need to calculate the Nusselt, Prandtl, and Reynolds numbers:

$$h = 129.8\; D^{-0.2}\, p^{0.8}\, T^{-0.55}\, v^{0.8} \tag{22}$$

$$v = C_1 . u \tag{23}$$

where p is pressure (in bar), T is the gas absolute temperature, u stands for the gas speed in the direction of compression, and $C_1 = 2.28$. This correlation has been developed to compute the convection heat transfer coefficient at the inner walls of tube-like pistons, considering the instantaneous gas temperature and pressure. Some adjustments were necessary due to our geometry and flow characteristics that differ from those of internal combustion engines for which the correlation was originally developed. The previous correlation was modified by using the hydraulic diameter as characteristic length:

$$D_{hyd} = \frac{4A}{P} \tag{24}$$

where A and P are respectively the area and the wetted perimeter of the cross-section of the liquid piston with inserted pipes. For C_1, a value of 12.5 was adopted for consistency with experimental and CFD data, what show to be in good agreement for a liquid piston without inserted tubes (Figs. 2 and 3.). The reason for the higher C_1 value when used in the liquid piston study is due to a more complex velocity field than that originally one studied by Wochini [22]. Since the calculation of the heat transfer coefficient is challenging and no standard approach is well-established for that, the present model uses only one global convection heat transfer coefficient instead of calculating three different ones for each heat transfer process in the LPC (Section 2.2). Thus, the heat transfer contribution of each single transfer process is not available. All the correlation adjustments make the model more useful and faster, and still gives excellent results when comparing with experimental and CFD results.

2.4. Compression efficiency and total efficiency

Two different efficiencies can be defined for the proposed LPC concept. The first one, η_1 (compression efficiency), indicates how close the actual compression is to the ideal isothermal compression process. It is defined as the ratio between the mechanical work required to compress a given mass of air from the same initial conditions to the same discharge pressure after an isothermal compression process and the

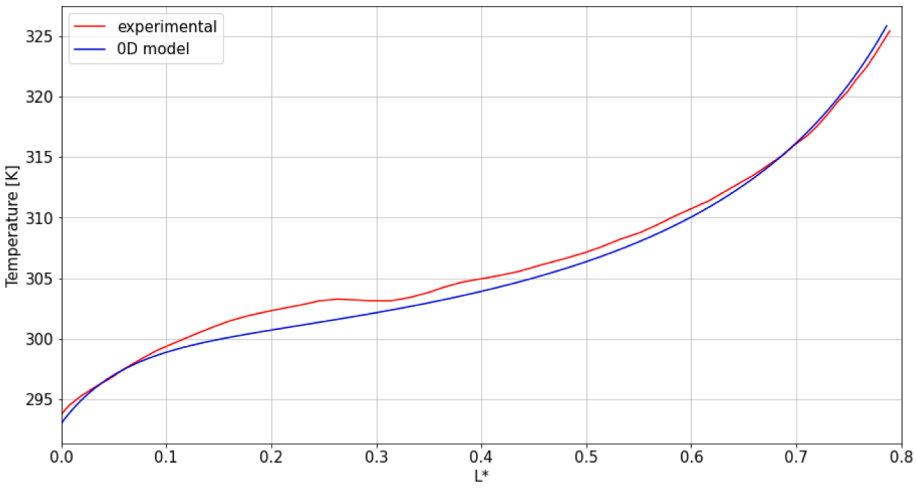

Fig. 2. Evolution of the average temperature as function of the piston location (present 0D results and experimental data from [17]).

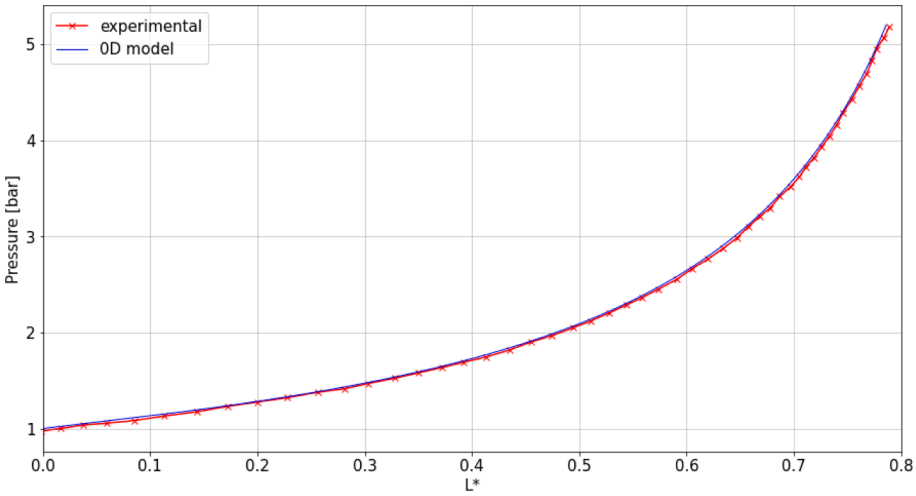

Fig. 3. Evolution of the gas pressure as function of the piston location (present 0D results and experimental data from [17]).

actual (non-isothermal) compression process:

$$\eta_1 = \frac{W_{isothermal}}{W_a} \tag{25}$$

where:

$$W_{isothermal} = p_0 V_0 ln\left(\frac{V_{fin}}{V_0}\right) = m_g R_g T_0 ln\left(\frac{p_{fin}}{p_0}\right) \tag{26}$$

V_{fin} is evaluated as:

$$V_{fin} = mR_g T_0 / p_{fin} \tag{27}$$

In both cases (isothermal and actual compression), the phase of discharge of the compressed gas at constant pressure is also considered. It should be noted that the final volume (or discharge volume, V_{fin}) is not the same for the (ideal) isothermal and for the real compression process (Eq. (27). W_a is the actual compression work required to compress and discharge the gas, which is calculated using the 0D model as

$$W_a = \dot{V}_g \int_{t_0}^{t_{fin}} (p_g - p_{atm}) dt \tag{28}$$

where $\dot{V}_g$ is equal to the (constant) water volume flow rate entering the liquid piston compression chamber.

The second efficiency, η_2 (total efficiency), quantifies how good the compression process is in general. Its definition includes the work required to compress the air, as well as the mechanical energy required to force the cooling fluid to flow in the cooling pipes and viscous losses in the compression chamber. This efficiency is defined as the ratio between the mechanical work required by the isothermal compression and the mechanical work required by the real compression cycle, that is:

$$\eta_2 = \frac{W_{isothermal}}{W_a + W_p + W_f} \tag{29}$$

The work spent to force the cooling liquid to flow in the cooling pipes is expressed as [23]:

$$W_p = n\Delta p \dot{V}_p t \tag{30}$$

where n is the number of cooling pipes, Δp the pressure drop along each of the cooling pipes, $\dot{V}_p$ the volume flow rate of the cooling liquid entering each of the cooling pipes and t the compression time (including the gas discharge phase). The cooling liquid pressure drop is evaluated as:

$$\Delta p = \rho_{cm} f \frac{L_p}{d_p} \frac{v_p^2}{2} \tag{31}$$

where ρ_{cm} is the density of the cooling medium, f is the friction factor, L_p and d_p are the pipe length and diameter, respectively, and v_p is the average speed of the cooling medium in the cooling pipes. For laminar

flow the friction factor is evaluated as:

$$f = \frac{64}{Re} \tag{32}$$

While for turbulent flow the explicit (approximate) Colebrook correlation may be applied, which, for internally smooth pipes, is:

$$f = 0.31/(log(0.143\,Re))^2 \tag{33}$$

Similarly, the equation for the mechanical work needed to overcome viscous friction in the compression chamber, W_f, can be derived. Two fluids are present (compressing gas and working liquid piston), whose viscous forces are causing mechanical losses. The pressure drop due to gas viscous forces are neglected, as its density is three orders of magnitude smaller than that of the liquid, and its dynamic viscosity is also considerably smaller than that of the liquid. Again, using Eqs. (31) to (33), replacing variables for properties of compression cylinder and numerically integrating the product of pressure drop (Δp) and the change in volume, W_f is obtained as:

$$W_f = \int_{t_0}^{t_k} \rho_{cf} f \frac{(L_p - z(t))}{D} \frac{v^2}{2} \dot{V} dt \tag{34}$$

where z is the current level of working liquid piston and $\dot{V}$, its volume flow rate.

3. Validation

3.1. Validation of the 0D model

In this section, the 0D calculations are validated by comparison with data from the literature. The used data set corresponds to the work of Neu and Subrenat [17]. Their experimental data were validated with the 0D analytical model under the same geometric and operational conditions. Air was compressing gas, and the compression column has 0.906 m long and 0.0518 m diameter. The velocity of the piston was 0.0333 m/s and the compression ratio is CR = 5.2, the compression process starting at atmospheric pressure. The time evolution of the average gas temperature and pressure was observed. The normalized length L^*:

$$L^* = \frac{L_{piston}}{L_{ch}} \tag{35}$$

where L_{piston} is the position of the piston that changes from the starting point ($L = 0$ m) to the point where the piston reaches the cylinder head ($L = L_{ch} = 0.906$ m) is used to represent the data.

In Fig. 2 the evolution of the temperature from the experiment is compared with 0D calculation. The original experimental data were averaged over 10 tests, the maximum temperature deviation being of 4.4 K. The 0D data and the experimental data show the same trend, with a maximum difference of less than 2.5 K at $L^* = 0.25$. This is less than the maximum deviation of the averaged 10 experimental tests [17]. The pressure curves in Fig. 3 show an almost perfect agreement.

3.2. Validation of the LPC containing cooling pipes – Comparison with the CFD results

To further test the results of the 0D approach and verify their reliability, a series of 3D CFD simulations was performed considering a cylindrical domain with a diameter $D = 0.0518$ m and inserted cooling tubes (see Fig. 1b). The length of the domain was corrected for each case to obtain the same initial mass of the gas starting with the air column with $L = 0.906$ m ($L/D = 17.5$). The 3D CFD calculations were performed using ANSYS Fluent v15. Despite low Reynolds numbers at initial conditions, a transition of the flow regime in the gas phase occurs during compression, as reported in the literature [18]. Therefore, LES model was used in combination with the PISO algorithm and the WALE sub-grid model to successfully model the laminar stage and local disturbances during the compression process, and to efficiently solve the unsteady Navier-Stokes equations. For these unsteady simulations, an adaptive time step was chosen and the control was adjusted to keep the global Courant number below 1. A constant temperature of 293 K and no slip wall boundary conditions were specified on the walls of the cylinder and outer walls of the cooling tubes. Air as ideal gas and water were used as the compressed gas and working and cooling fluid. The VOF model was used to simulate the two phases flow in the cylinder (compression chamber) enclosure. Constant water velocity of 0.033 m/s and temperature of 293 K were assigned at the inlet. Air pressure and temperature were initialized with the ambient values of 101325 Pa and 293 K, respectively. Simulations were finished once reached a compression ratio of 5.

The study of the mesh independence was performed considering 3 different meshes containing only hexahedral elements. The number of elements in the coarse mesh was 0.6×10^6 (Fig. 4), in the medium mesh 1.2×10^6, and in the fine mesh 2×10^6. The average temperature (Fig. 5) was chosen for mesh comparison results because it presents larger differences than pressure. Coarse mesh presents less than 0.5 K maximum temperature difference from fine mesh, the maximum temperature difference of the medium mesh being smaller than 0.2 K. This indicates that influence of number of mesh elements is in fact small between the middle and finer meshes. Density of middle mesh was chosen for the rest of the computations, representing a good balance between the results accuracy and the required calculation time.

The results were obtained considering 3 different numbers of cooling tubes: 0 (no cooling tubes), 4 and 8 cooling tubes, with an outer diameter of 10 mm. The pressure and temperature results of the 3D CFD and the 0D model are shown in Figs. 6 and 7. As it can be seen in Fig. 6, pressure increases continuously with time until the limiting discharge pressure is reached. It can be seen that the trends are the same for all cases, only the time to reach the discharge pressure increases for higher number of cooling pipes. The results of CFD and the 0D calculation perfectly overlap for 0 inserted cooling tubes. For 4 and 8 inserted cooling pipes, pressure curve rises slower in first part for results obtained using the 0D model. Maximum deviation between CFD and 0D calculated pressure data for 8 inserted cooling tubes is less than 0.2 bar at $t = 28.5$ s. After it CFD curve rises steeper, reaching the discharge pressure 0.15 s slower than the 0D calculated compression. For 4 inserted cooling tubes the maximum deviation between the CFD simulated and 0D calculated results is of 0.2 bar at $t = 8.2$ s. The temperature results in the case of the CFD study are calculated as the element volume average temperature in the cylinder domain. As can be seen in Fig. 7, the air temperature increases as air compression progresses, a similar trend of temperature increase being observed for any number of inserted cooling tubes. It is clear that the insertion of cooling tubes promotes heat

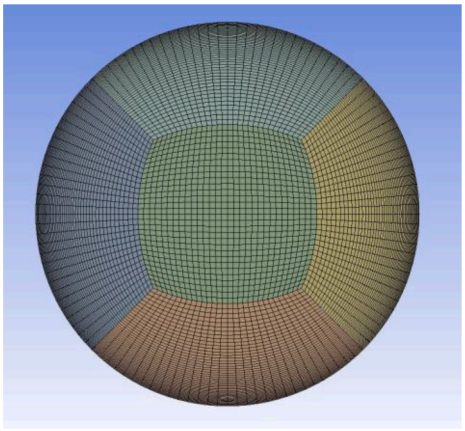

Fig. 4. Coarse hexahedral type mesh used for CFD calculations – 0 inserted pipes.

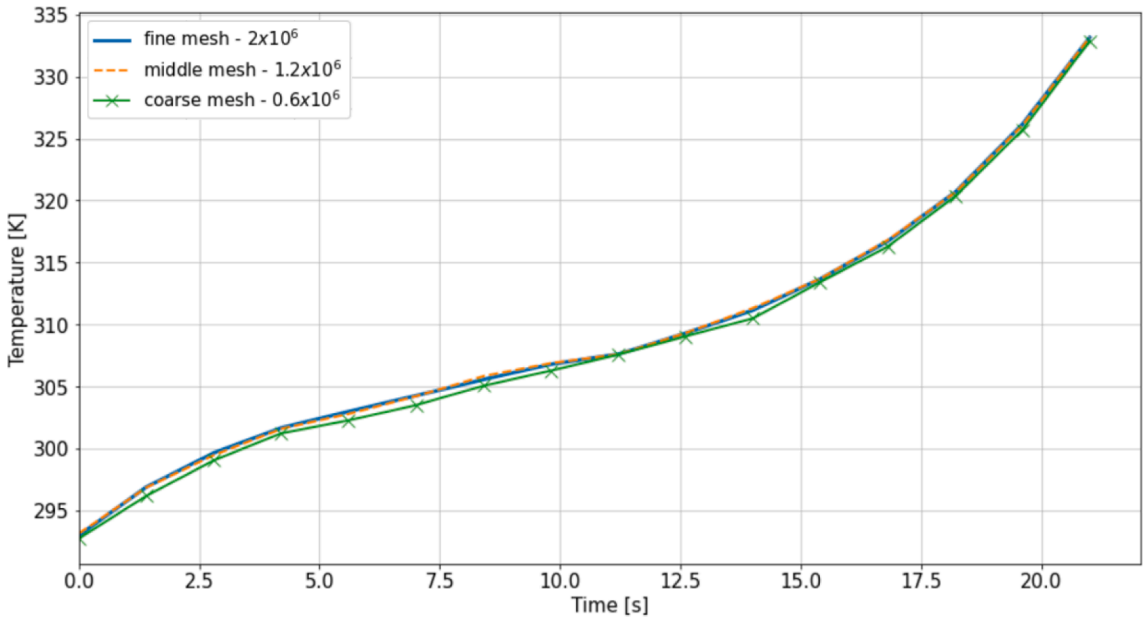

Fig. 5. Time evolution of average temperature in the compression chamber with coarse, medium and fine mesh – CFD calculations.

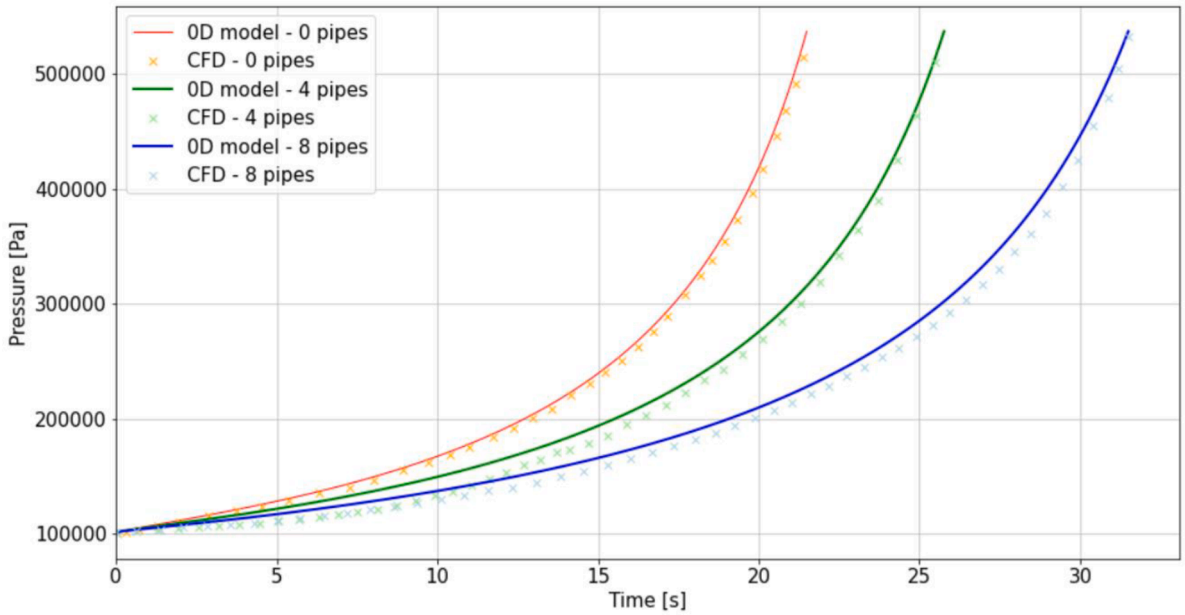

Fig. 6. Effect of the number of cooling pipes on the air pressure time evolution (0D model approach and 3D CFD results for $d_p = 10$ mm, $v = 0.033$ m/s, $v_{cf} = 0.3$ m/s, L/D (0 inserted tubes) = 17.5, $CR = 5.3$.

transfer and makes the compression in the LPC more isothermal. Inserting 4 cooling tubes, the final temperature drops by 21 K, and drops by 31 K if 8 cooling tubes are inserted. Both the data generated by CFD and by the 0D model show the same trends and final gas temperatures. The 0D approach calculates slightly higher temperatures in the first half of the compression process, but the deviation still remains below 1 K.

In Fig. 8 and 9 are represented the velocity and temperature CFD contours for cases with 0, 4 and 8 cooling pipes at different compression stages. In Fig. 8a we can observe perturbations of velocity in compressing gas and laminar flow of the liquid phase. At the same time, oscillations can be seen also in the temperature contours (Fig. 9a). Brighter contours near the cylinder walls and near the gas–liquid interface represent areas where heat is removed more effectively. The highest temperatures are observed near the top wall, where an adiabatic boundary condition was prescribed. Laminar regime of compression can be seen in Figs. 8b and 9b. The flow is axisymmetric and no perturbations can be identified as compression is in early stages. Velocity is highest in the area between the cooling tubes, where the cross-section for the gas to flow is largest. Where velocity is highest, the local air is compressed the most and therefore its temperature rise is higher than elsewhere in the domain. In Figs. 8c and 9c compression is in final stages, and perturbations can be seen in the velocity and temperature contours. Highest temperatures and velocities occur in pockets between the outer cooling tubes and the cylinder wall.

3.3. Cooling fluid temperature

For the CFD simulations, a constant wall temperature of the cylinder

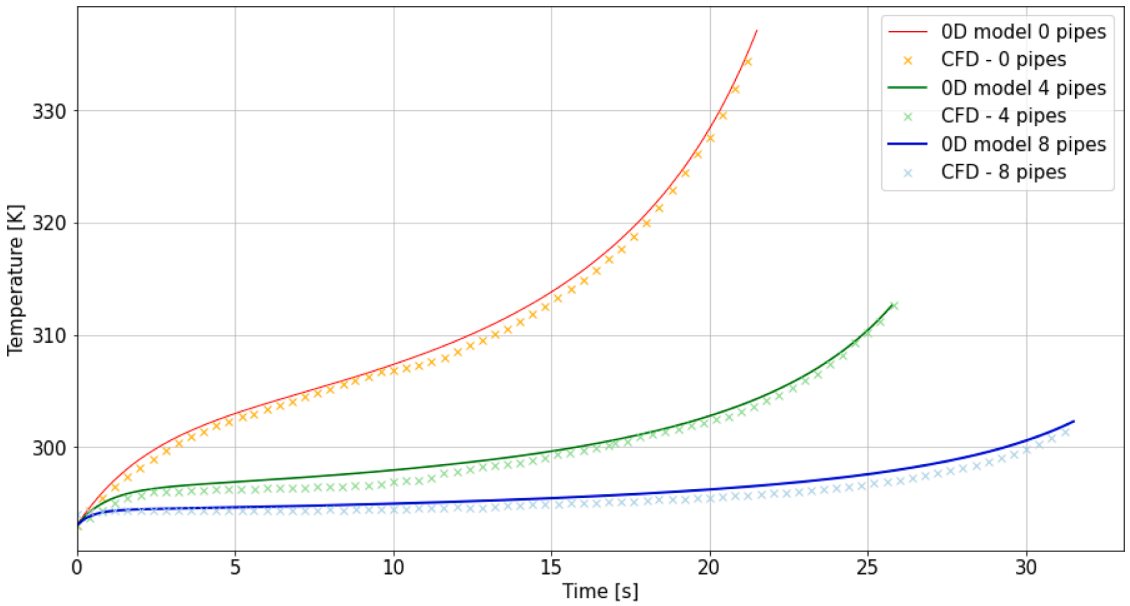

Fig. 7. Effect of the number of cooling pipes on the average air temperature time evolution (0D model approach and 3D CFD results, for $d_p = 10$ mm, $v = 0.033$ m/s, $v_{cf} = 0.3$ m/s, L/D (0 inserted tubes) $= 17.5$, $CR = 5.3$.

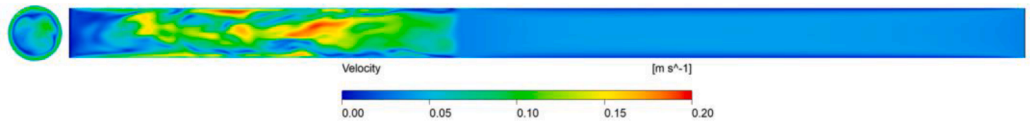

Fig. 8a. Gas velocity contours at $t = 15$ s, cross section at 0.1 m from the top wall, 0 cooling tubes, $v = 0.033$ m/s, $L/D = 17.5$.

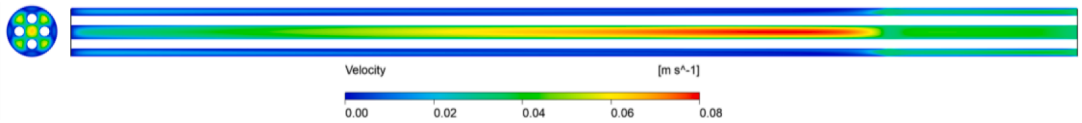

Fig. 8b. Gas velocity contours at $t = 5$ s, cross section at 0.1 m from the top wall, 4 cooling tubes, $d_p = 10$ mm, $v = 0.033$ m/s, L/D (0 inserted tubes) $= 17.5$.

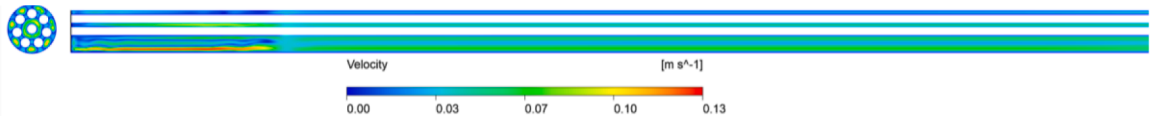

Fig. 8c. Gas velocity contours at $t = 31$ s, cross section at 0.1 m from the top wall, 8 cooling tubes, $d_p = 10$ mm, $v = 0.033$ m/s, L/D (0 inserted tubes) $= 17.5$.

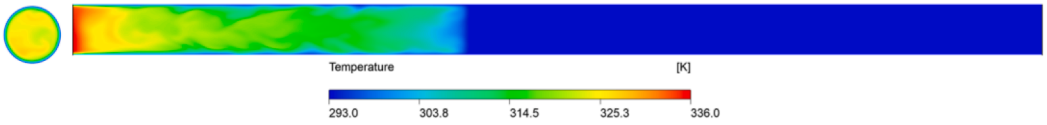

Fig. 9a. Gas temperature contours at $t = 15$ s, cross section at 0.1 m from the top wall, 0 cooling tubes, $v = 0.033$ m/s, $L/D = 17.5$.

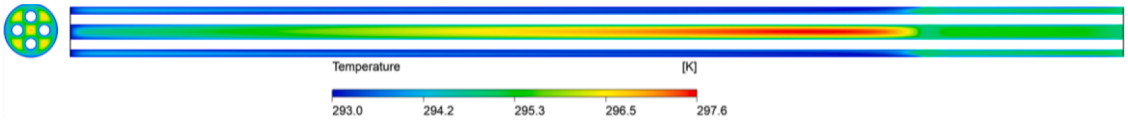

Fig. 9b. Gas temperature contours at $t = 5$ s, cross section at 0.1 m from the top wall, 4 cooling tubes, $d_p = 10$ mm, $v = 0.033$ m/s, L/D (0 inserted tubes) $= 17.5$.

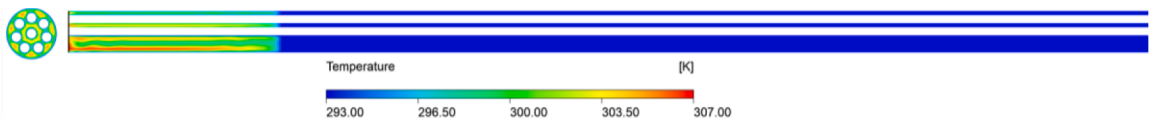

Fig. 9c. Gas temperature contours at t = 31 s, cross section at 0.1 m from the top wall, 8 cooling tubes, d_p = 10 mm, v = 0.033 m/s, L/D (0 inserted tubes) = 17.5.

was chosen as the thermal boundary condition, assuming that the cylinder is immersed in a liquid basin and that the surrounding cooling water can maintain this temperature. To confirm that the cooling fluid in the tubes is capable of removing most of the heat released by the compressing gas, the temperature rise of the cooling fluid was calculated. In addition, two CFD simulations were performed in which the fluid in the cooling tubes was also simulated. The heat transfer between the compressing gas and the cooling liquid was coupled without considering the tube walls, resulting in conditions similar to those in the 0D model. Fig. 10 shows the values of the average temperature of the cooling liquid at the outlet of the cooling tubes during compression for two different numbers of tubes (4 and 8), which shows that the temperature of the cooling liquid is indeed almost uniform. CFD results show a similar trend of average temperature at the outlet of the tubes. A constant volume flow rate of 0.054 m^3/h of cooling water in one cooling tube was chosen, corresponding to a flow velocity of 0.3 m/s in a tube with 8 mm internal diameter. The initial temperature was set as being 293 K. It can be observed that the temperature of the cooling water does not increase as much when 8 cooling tubes are used as when 4 cooling tubes are used. This is due to the smaller temperature rise of the compressing gas and the larger amount of water used to cool the tube walls. Despite the large assumption of the temperature distribution in the area of the cooling tubes (Eq. (14), excellent agreement with the CFD results can be observed, so such an assumption seems to be reasonable. Increasing the temperature of the cooling liquid decreases the overall efficiency of the compression, as does a higher volume flow rate of the cooling water in the cooling tubes, which must be carefully chosen to ensure the highest LPC efficiency. At the selected value of the cooling water volume flow rate (0.054 m^3/h in a single cooling tube), the temperature of the cooling water increases only by 0.047 K and by 0.031 K for the cases with 4 and 8 cooling tubes used, respectively, which means effective cooling and adequate volumetric flow rate of the cooling water.

3.4. Efficiency and work of the liquid piston with inserted pipes

Both compression efficiency and total efficiency and all work types referred in Section 2.4 were calculated using the 0D and CFD approaches.

The role of the number of cooling tubes was analysed using the 0D model by considering a range from 0 to 20 tubes with an outer diameter of 10 mm and an inner diameter of 8 mm. Again, the velocity of the cooling water was set to 0.3 m/s, resulting in a volumetric flow rate of 0.054 m^3/h in one tube. The dependence of the work required for the isothermal and the actual compressions on the number of cooling tubes can be seen in Fig. 11a. Since the mass of the compressing gas and the initial and final pressures are the same in all the cases considered, the value of the work required for isothermal compression ($W_{isotherm}$) is the same, which allows us to calculate the efficiencies for the different cases without bias. The work required for the compression of air (W_a) decreases as the number of cooling tubes increases, following the expected effect from the increased contact area and convection heat transfer coefficient, thus more effectively lowering the temperature of the gas being compressed. The calculated mechanical work to overcome the viscous friction of the fluid in the cylinder housing of the liquid piston (W_f) is very low (in the range of 10^{-3} J) in all areas of the inserted cooling tubes and increase slightly with the number of cooling tubes (Fig. 11b). This is the contribution of the contact area between the fluid and the rigid walls, increasing the viscous friction and causing increased mechanical losses. Due to the higher number of inserted cooling tubes, the total volume flow rate of the cooling fluid increases and so does the mechanical work spent to force the flow in the cooling tubes (W_p). Fig. 11c shows the comparison between the compression efficiency (η_1) and the total efficiency (η_2). For 0 inserted cooling tubes, the values overlap since there are no losses in the tubes and the viscous losses of the compressing fluid are almost negligible. As expected, the overall efficiency is smaller than the compression efficiency. The reason for that is the work required to get the cooling water flowing in the cooling tubes.

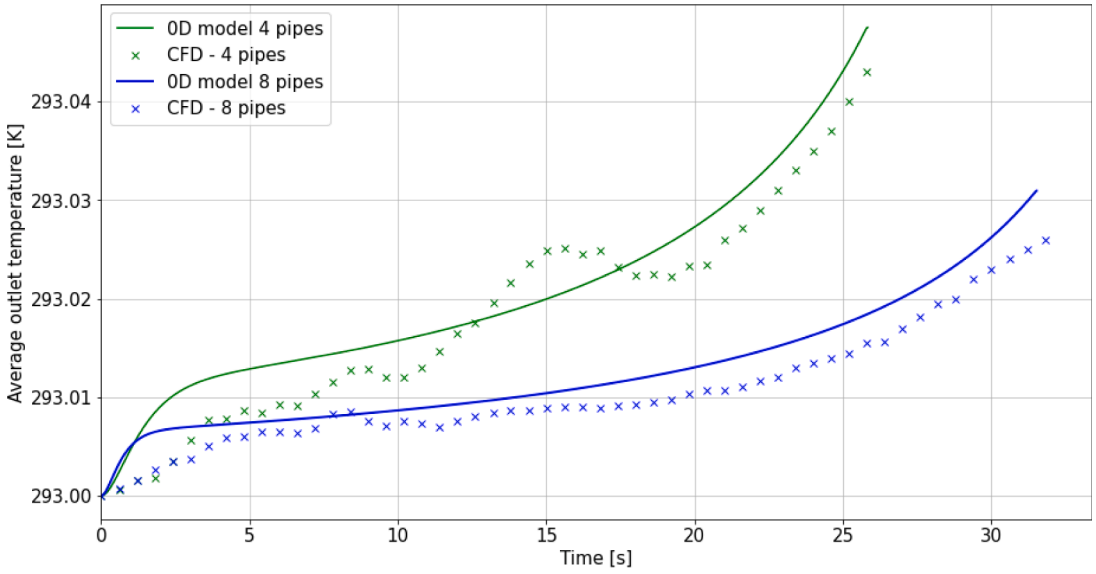

Fig. 10. Effect of the number of cooling pipes on the time evolution of the temperature increase of the cooling fluid at the tubes outlet (0D model approach and 3D CFD results, for d_p = 10 mm, v = 0.033 m/s, v_{cf} = 0.3 m/s, L/D (0 inserted tubes) = 17.5, CR = 5.3.

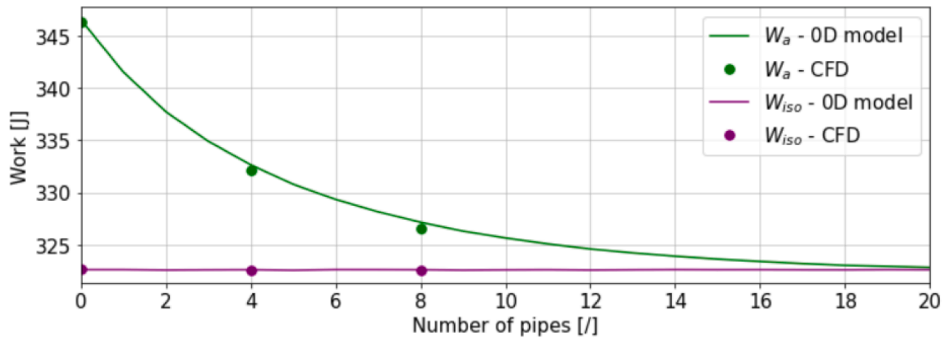

a)

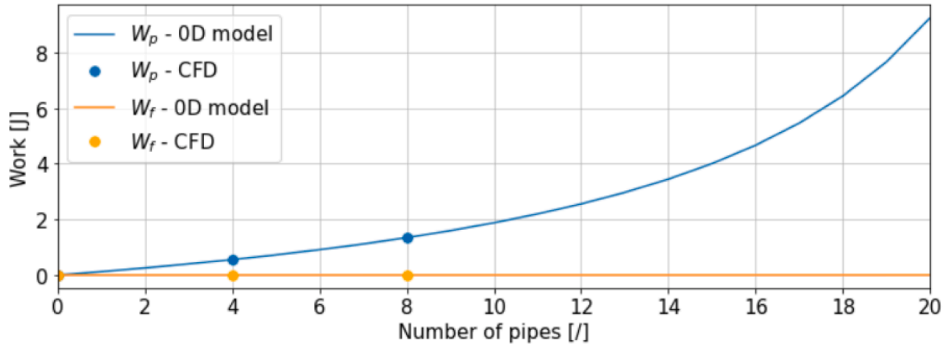

b)

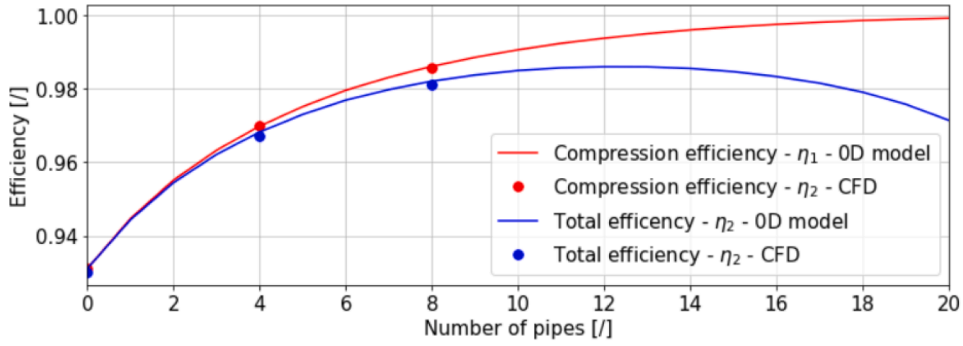

c)

Fig. 11. 0D model approach and CFD results of the: a) Actual compression work and the isothermal compression work; b) Frictional work in the cylinder and the work required to circulate the cooling fluid; and c) Total and the compression efficiency versus the number of cooling pipes, for $d_p = 10$ mm, $v = 0.033$ m/s, $v_{cf} = 0.3$ m/s, L/D (0 inserted tubes) = 17.5, $CR = 5.3$.

The pumping power increases with the number of cooling tubes, which increases the difference between the compression efficiency and the total efficiency, and also decreases the peak value of the total efficiency. As the number of inserted tubes increases, the compression efficiency asymptotically approaches the value of 1. The total efficiency, on the other hand, shows lower values and falls after the peak value. After that, W_p rises faster than W_a falls. The peak value of the overall efficiency (η_2) is of 98.6% for 12 cooling tubes, what means that this liquid piston arrangement is the most efficient with the parameters of cylinder diameter, length, liquid piston velocity and cooling liquid velocity used. The points on the curves represent the calculated values of work and efficiency from the CFD simulations. All points show a good agreement with the results obtained using the simplest 0D model approach.

4. Parametric optimisation

Since there is a good agreement between the 0D and 3D CFD results, confident data can be obtained using the simpler 0D model approach for parametric optimization of LPCs.

To arrive as close as possible to an isothermal compression process, the parametric optimization should focus on low compression ratios and low compression velocities, as well as on long cylinder compression chambers with small diameters (large L/D ratios). Under these conditions, long cycles are required in which only small amounts of air are compressed, resulting in compression processes with low power densities. The same happens with the cooling tubes - a large number of cooling tubes makes the compression more isothermal, but reduces the available space for the amount of air to be compressed in the compression chamber. This leads to an optimization problem with a large number of governing parameters (diameter and length of the

compression chamber, liquid piston velocity, compression ratio, number of cooling tubes, diameter of the cooling tubes and velocity (or flow rate) of the cooling liquid). In addition, other parameters can be considered and optimised, such as the shape of the cylindrical compression chamber [24] and the liquid pumping trajectory [25]. Thus, the optimization of LPCs can become a rather complex problem, and the results should be sought considering the intended use, the dimensions of the system, and (with respect to the real LPC) the required manufacturing processes.

In what follows the behaviour of the LPC system as a function of the number and diameter of the cooling tubes is presented. A new method for the optimization of LPC with inserted cooling tubes is described. Due to the large number of governing parameters, some of them must be determined in a first step. First of all, the mass of the compressing gas and the compression ratio (CR) must be determined so that the same value of isothermal work ($W_{isothermal}$) and the same amount of compressed gas produced are used when comparing different LPC configurations and operating conditions. Length (L) and diameter (D) of the compression chamber are the basic parameters to define the mass of the gas to be compressed. Therefore, in a first step, the optimization starts with a chosen value of these parameters, which must meet the requirements of installation, manufacturability and gas discharge pressure. The length is then adjusted so that the LPC with the selected number of inserted cooling tubes can hold the same mass of gas to be compressed. The velocity of the cooling liquid is chosen so that the outer walls of the cooling tubes are at nearly the constant initial temperature. The only variable parameters that remain are thus the number of cooling tubes (N_p), the diameter of the cooling tubes (d_p) and the velocity of the liquid piston (v). The number of cooling tubes is limited by the chosen diameter of the cylindric compression chamber, since there is a maximum value of inserted cooling tubes for a given diameter of the compression chamber. For this purpose, the maximum number of inserted cooling tubes for a given diameter of the compression chamber was calculated by solving the circle packing problem [26] using an available calculator for that [27]. Moreover, the maximum and minimum diameter of the cooling tubes is limited by the diameter of the base cylinder and the thickness of their walls, respectively.

All calculations were performed for a cylinder with length $L = 0.906$ m and diameter $D = 0.0518$ m, giving a L/D for the base case (0 inserted cooling tubes) of 17.5. The minimum diameter of the cooling tubes was set to 4 mm and the wall thickness was made equal to 1 mm for all diameters considered. The maximum diameter of the cooling tubes was set to 14 mm. The maximum number of cooling tubes varies from 9 (for the largest considered diameter) up to 127 (for the smallest considered diameter).

The effect of the number and diameter of cooling tubes on the total efficiency is shown in Fig. 12. With larger cooling tube diameters, fewer cooling tubes are needed to achieve the same total efficiency. Also, the peak of the total efficiency is higher when larger diameter cooling tubes are used. The number of cooling tubes for peak efficiency decreases with larger diameter cooling tubes. As mentioned earlier, when more cooling tubes are used to accommodate the same mass and initial gas volume, the cylinder enlarges, increasing the time required for compression. As can be seen in Fig. 13, the compression time for the most efficient case increases for larger diameters. In Fig. 14 are shown results for combinations of the numbers of tubes and their diameters for the most efficient cases. A very interesting phenomenon can be seen in Fig. 15, where the total efficiency η_2 is plotted as function of the number of cooling tubes for 3 different velocities of the liquid piston for the same diameter (of 6 mm) of the cooling tubes. For a number of inserted cooling tubes between 0 and 15, the slow compression is more efficient. At slower compression velocities there is more time for heat transfer from the gas, resulting in a more isothermal compression. The trend changes for more than 15 inserted cooling tubes, for which a faster compression is more efficient. In the cases shown in Fig. 15, the same amount of gas is always compressed. This means that with a faster compression we can produce larger volumes of compressed gas with the same or even better efficiency. It follows that the efficiency also contains information about the compression time, and that above 15 cooling tubes contribution of faster compression is higher than the lowering final temperature of a single stroke associated with a slower compression.

The 0D model can be confidently used for LPC optimization,taking advantage of its simplicity, faster calculations, and reduced need of calculation resources, making it the most adequate approach to deal with the large number of cases with different parameters that need to be considered. This is the case of the above-mentioned optimization, which required a total of 642 cases simulations. From Figs. 12, 14 mm cooling tubes lead to the highest total efficiency. If we focus on the mentioned diameter in Fig. 13, liquid piston velocity of 0.0666 m/s allows the shortest compression time of one stroke. For this combination of diameter and velocity, the number of cooling tubes (9) that leads to the highest efficiency can be read out from Fig. 14. From all calculated cases, the most efficient combination corresponds to 9 cooling tubes with a diameter of 14 mm, and a liquid piston velocity of 0.066 m/s. Air in this case is compressed in 32 s, and the total efficiency of the process is calculated to be 99.3 %. The final step of the optimization represents the optimization of the cooling fluid velocity. By lowering its value, we can achieve even higher values of the total efficiency, the only thing that should be taken into account being the associated increase in the temperature of the cooling fluid and, consequently, the possibility of an increase in the temperature of the compressed gas. In this case, the compression would be more far from the isothermal compression, and the efficiency decreases.

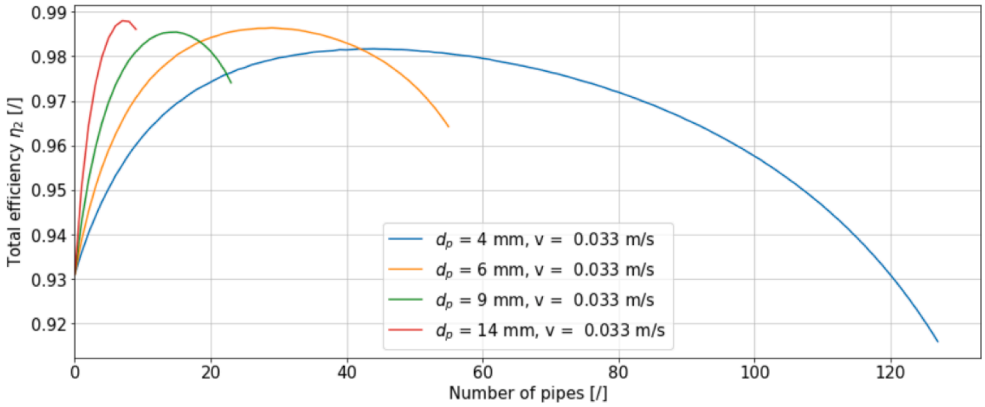

Fig. 12. Total efficiency as function of the number of cooling pipes for 4 different diameters of inserted cooling tubes, for $v = 0.033$ m/s, $v_{cf} = 0.3$ m/s, L/D (0 inserted tubes) = 17.5, $CR = 5.3$.

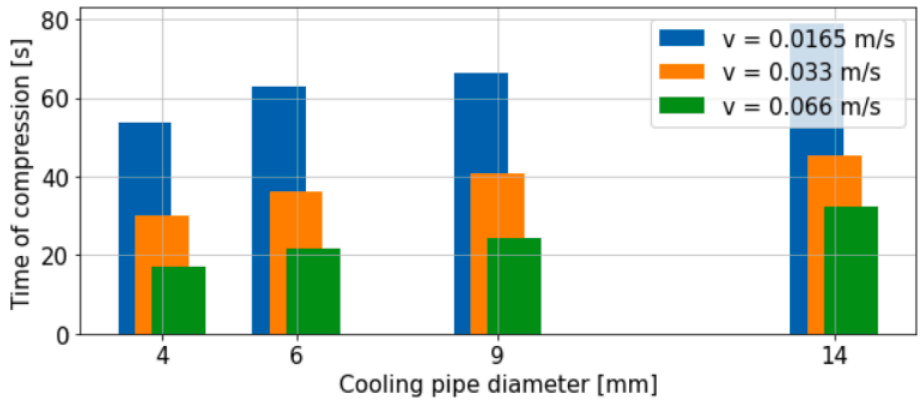

Fig. 13. Time of compression for the most efficient number of cooling tubes for 4 different diameters and 3 different liquid piston velocities, for $v_{cf} = 0.3$ m/s, L/D (0 inserted tubes) = 17.5, $CR = 5.3$.

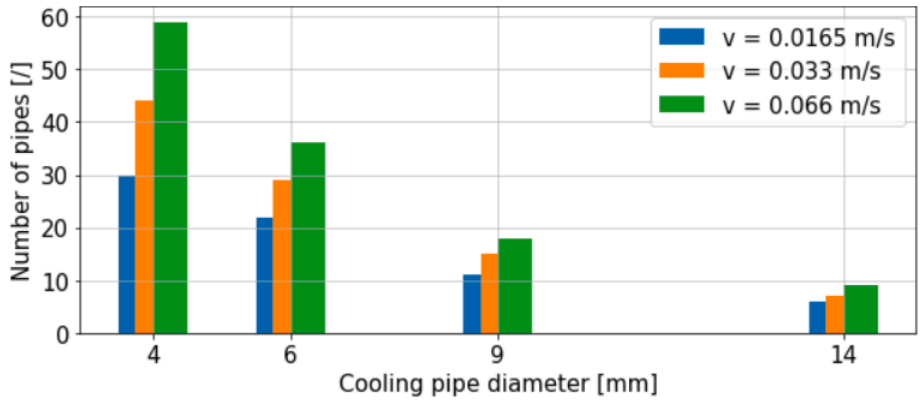

Fig. 14. Number of cooling pipes for the most efficient cases for 4 different cooling tubes diameters and 3 different liquid piston velocities, for $v_{cf} = 0.3$ m/s, L/D (0 inserted tubes) = 17.5, $CR = 5.3$.

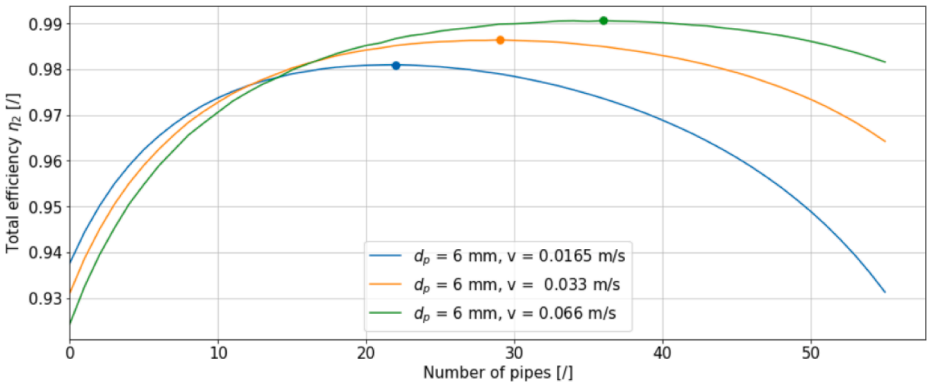

Fig. 15. Total efficiency as function of the number of inserted cooling tubes with a diameter of 6 mm for 3 different liquid piston velocities, for $d_p = 6$ mm, $v_{cf} = 0.3$ m/s, L/D (0 inserted tubes) = 17.5, $CR = 5.3$.

5. Conclusions

Liquid piston compression is a promising technique for gases compression, due to the absence of moving mechanical parts and gas leakage in the piston. Moreover, because of the inherent flexibility in what concerns geometrical configuration of the compression chamber, it is possible to obtain an increased heat transfer from the compressing gas, thus allowing a more isothermal compression process. The compression process should be as isothermal as possible and, for that purpose, the present work proposes a LPC that consists on a cylindrical compression chamber with a set of inserted cooling pipes. Such LPCs are easy to manufacture: simple pipes can be welded in a cylindrical shaped metal vessel, using only common materials with common cylindrical shapes. There is no need to regenerate the cooling inserts from compression cycle to compression cycle, thanks to the continuously flowing cooling medium.

The compression efficiency was modelled as a function of the LPC governing parameters, namely the compression ratio, the liquid piston displacement velocity, the cylinder aspect ratio L/D, the number and diameter of cooling pipes, and the velocity of the cooling fluid. A 0D model was proposed for evaluation of the gas temperature and pressure time evolutions during the compression process, for both the

compression chamber without and with inner cooling pipes. The model was validated with available experimental data and conducted 3D CFD simulations. The proposed 0D model was used in systematic parametric optimization studies to reveal the separate and combined influence of the governing parameters on compression efficiency.

The proposed 0D model includes assumptions to make computations and LPCs behaviour prediction simpler. Uniform compression velocities and wall temperatures were considered, even if they may slightly change under real operating conditions. There are also losses in valves and hazard of gas entering the compressing liquid. Calculation of the convection heat transfer coefficient is a complex problem, as it depends on geometrical and operational parameters. Nevertheless, the presented 0D model can be used for fast generation of data to optimise LPCs, and therefore to design, test and built effective LPCs for gases compression.

The main results of this study can be summarized as:

- The total efficiency presents a maximum for a given number of cooling pipes. A lower number of cooling pipes leads to a less effective heat removal rate from the compressing gas. A higher number of cooling pipes leads to a more effective heat removal rate from the compressing gas, but leads also to higher head losses in the cooling pipes and viscous losses in the cylinder, thus decreasing the total efficiency;
- The maximum total efficiency is higher for fewer and larger cooling pipes diameters, due to the high heat transfer surface area and lower head losses. The associated drawback of using fewer and larger cooling pipes diameters is the lower air mass being compressed in each compression stroke in same cylinder enclosure, slowing the overall compression process due to the larger number of compression strokes required.
- At lower piston speeds there is more time for heat transfer from the compressing gas, thus allowing more near-isothermal compression and rising efficiency, but with inserted cooling pipes, which reduces mass of intake gas, effect of higher liquid piston speeds can lead to increased efficiency as more gas can be compressed in the same time.
- Total efficiency can be further increased by optimising the volume flow rate of the cooling medium, balancing between lowering the head losses and reducing the positive effect of cooling the compressing gas. This is more relevant for higher numbers of successive compression strokes.

An experimental study of the proposed LPC concept would be necessary, to further validate and investigate the convection heat transfer coefficient correlation, 0D model and findings of parametric optimisation. Modelling of wider system, taking into account all connecting pipes, pumps, valves and liquid leakage would help to calculate total efficiency more accurately. Flow and heat transfer in inserted cooling tubes and their walls must be further researched to confirm the effectiveness of proposed concept. As flow over tubes can induce vibrations, also a mechanical dynamic study of proposed concept would be necessary towards more robust and reliable designs of LPCs that can be applied in industry, and in energy production and storage.

CRediT authorship contribution statement

N. Cerkovnik: Methodology, Investigation, Writing – original draft. **V.A.F. Costa:** Conceptualization, Methodology, Writing – review & editing. **A.M.G. Lopes:** Conceptualization, Resources, Writing – review & editing, Supervision.

Declaration of Competing Interest

The authors declare that they have no known competing financial interests or personal relationships that could have appeared to influence the work reported in this paper.

Data availability

Data will be made available on request.

Acknowledgements

This work was supported by the projects UIDB/00481/2020 and UIDP/00481/2020, Fundação para a Ciência e a Tecnologia (FCT) and CENTRO-01-0145-FEDER-022083, Centro Portugal Regional Operational Programme (Centro2020), under the PORTUGAL 2020 Partnership Agreement, through the European Regional Development Fund.

References

[1] N.H. Stern, The Economics of Climate Change: The Stern Review, Cambridge University Press, Cambridge, UK, 2007.
[2] M. Specklin, M. Deligant, P. Sapin, M. Solis, M. Wagner, C.N. Markides, F. Bakir, Numerical study of a liquid-piston compressor system for hydrogen applications, Appl. Therm. Eng. 216 (2022) 118946.
[3] H. Zhou, P. Dong, S. Zhu, S. Li, S. Zhao, Y. Wang, Wang Y, Design and theoretical analysis of a liquid piston hydrogen compressor, J. Storage Mater. 41 (2021) 102861.
[4] P. Murti, E. Shoji, T. Biwa, Analysis of multi-cylinder type liquid piston Stirling cooler, Appl. Therm. Eng. 219 (2023) 119403.
[5] R. Chouder, A. Benabdesselam, P. Stouffs, Modeling results of a new high performance free liquid piston engine, Energy 263 (2023) 125960.
[6] M. Mutlu, M. Kiliç, Effects of piston speed, compression ratio, and cylinder geometry on system performance of a liquid piston, Therm. Sci. 20 (6) (2016) 1953–1961.
[7] T. Neu, C. Solliec, B. dos Santos Piccoli, Experimental study of convective heat transfer during liquid piston compressions applied to near isothermal underwater compressed-air energy storage, J. Storage Mater. 32 (2020) 101827.
[8] C. Qin, E. Loth, Liquid piston compression efficiency with droplet heat transfer, Appl. Energy 114 (2014) 539–550, https://doi.org/10.1016/j.apenergy.2013.10.005.
[9] J.D. Van de Ven, P.Y. Li, Liquid piston gas compression, Appl. Energy 86 (10) (2009) 2183–2191, https://doi.org/10.1016/j.apenergy.2008.12.001.
[10] V.C. Patil, J. Liu, P.I. Ro, Efficiency improvement of liquid piston compressor using metal wire mesh for near-isothermal compressed air energy storage application, J. Energy Storage 28 (2020), 101226, https://doi.org/10.1016/j.est.2020.101226.
[11] B. Yan, J.H. Wieberdink, F.A. Shirazi, P.Y. Li, T.W. Simon, J.D. Van de Ven, Experimental study of heat transfer enhancement in a liquid piston compressor/expander using porous media inserts, Appl. Energy 154 (2015) 40–50, https://doi.org/10.1016/j.apenergy.2015.04.106.
[12] C. Zhang, B. Yan, J. Wieberdink, P.Y. Li, J.D. Van de Ven, E. Loth, T.W. Simon, Thermal analysis of a compressor for application to Compressed Air Energy Storage, Appl. Therm. Eng. 73 (2014) 1402–1411, https://doi.org/10.1016/j.applthermaleng.2014.08.014.
[13] A. Odukomaiya, A. Abu-Heiba, K.R. Gluesenkamp, O. Abdelaziz, R.K. Jackson, C. Daniel, S. Graham, A.M. Momen, Thermal analysis of near-isothermal compressed gas energy storage system, Appl. Energy 179 (2016) 948–960, https://doi.org/10.1016/j.apenergy.2016.07.059.
[14] V.C. Patil, P.I. Ro, Experimental study of heat transfer enhancement in liquid piston compressor using aqueous foam, Appl. Therm. Eng. 164 (2020) 114441.
[15] K.R. Ramakrishnan, P.I. Ro, V.C. Patil, Temperature abatement using hollow spheres in liquid piston compressor for ocean compressed air energy storage system, in: OCEANS 2016 MTS/IEEE Monterey, OCE 2016, IEEE, 2016, pp. 1–5, https://doi.org/10.1109/OCEANS.2016.7761341.
[16] V.C. Patil, P. Acharya, P.I. Ro, Experimental investigation of heat transfer in liquid piston compressor, Appl. Therm. Eng. 146 (2019) 169–179, https://doi.org/10.1016/j.applthermaleng.2018.09.121.
[17] T. Neu, A. Subrenat, Experimental investigation of internal air flow during slow piston compression into isothermal compressed air energy storage, J. Storage Mater. 38 (2021) 102532.
[18] E.M. Gouda, M. Benaouicha, T. Neu, Y. Fan, L. Luo, Flow and heat transfer characteristics of air compression in a liquid piston for compressed air energy storage, Energy 254 (2022) 124305.
[19] E.M. Gouda, Y. Fan, M. Benaouicha, T. Neu, L. Luo, Fan Y, Benaouicha M, Neu T, Luo L, Review on Liquid Piston technology for compressed air energy storage, Journal of Energy Storage 43 (2021) 103111.
[20] Piya C., Sircar I., Van de Ven J.D., Olinger D.J., Numerical Modeling of Liquid Piston Gas Compression, Proceedings of ASME 2009 2009 ASME International Mechanical Engineering Congress and Exposition November 13-19, 2009, Lake Buena Vista, Florida, USA, IMECE2009-10621.
[21] Tuhovcák J, Hejík J, Jícha M, "Heat Transfer Analysis in the Cylinder of Reciprocating Compressor" (2016). International Compressor Engineering Conference. Paper 2409. https://docs.lib.purdue.edu/icec/2409.
[22] G. Woschini, A Universally Applicable Equation for the Instantaneous Heat Transfer Coefficient in the Internal Combustion Engine, SAE Transactions 76 (1968), pp. 3065-3083, https://www.jstor.org/stable/44562845.
[23] B. Kraut, et al., Krautov strojniški priročnik, Univerza v Ljubljani, Fakulteta za strojništvo, 2021 https://scholar.google.com/citations?view_op=view_

citation&hl=en&user=fFd3QCAAAAAJ&citation_for_view=fFd3QCAAAAAJ:MXK_kJrjxJIC.
[24] C. Zhang, P.Y. Li, J.D. Van de Ven, T.W. Simon, Design analysis of a liquid-piston compression chamber with application to compressed air energy storage, Applied Thermal Engineering 101 (2016) 704–709.
[25] Saadat, PYL, Simon TW, Optimal trajectories for a liquid piston compressor/expander in a compressed air energy storage system with consideration of heat transfer and friction, in: Proceedings of the American Control Conference, IEEE, 2012, pp. 1800–1805, https://doi.org/10.1109/acc.2012.6315616.
[26] R.L. Graham, B.D. Lubachevsky, K.J. Nurmela, P.R.J. Östergård, Dense packings of congruent circles in a circle, Discret. Math. 181 (1998) 139–154, https://doi.org/10.1016/S0012-365X(97)00050-2.
[27] Engineering ToolBox, (2013). Smaller Circles within a Larger Circle - Calculator. [online] Available at: https://www.engineeringtoolbox.com/smaller-circles-in-larger-circle-d_1849.html [Accessed 8. 12. 2022].